TECHNICAL NOTE

Cytometry PART A
Journal of the International Society for Advancement of Cytometry

Improved Detection of Nicotinamide Adenine Dinucleotide Phosphate Oscillations Within Human Neutrophils

Andrea J. Clark,[1] Roberto Romero,[2,3,4] Howard R. Petty[1,5]*

[1]Department of Ophthalmology and Visual Sciences, The University of Michigan Medical School, Ann Arbor, MI

[2]Perinatology Research Branch, Division of Intramural Research, Eunice Kennedy Shriver National Institute of Child Health and Human Development (NICHD) of NIH, Bethesda, Maryland, and Detroit, Michigan

[3]Center of Molecular Medicine and Genetics, Wayne State University, Detroit, Michigan

[4]Hutzel Women's Hospital at the Detroit Medical Center, Detroit, Michigan

[5]Department of Microbiology and Immunology, The University of Michigan Medical School, Ann Arbor, MI

Received 19 March 2010; Revision Received 24 June 2010; Accepted 23 July 2010

Grant sponsor: Division of Intramural Research of the Eunice Kennedy Schriver National Institute of Child Health and Human Development, NIH, DHHS; Grant numbers: contract N01-HD-2-3342 and subcontract WSU04055.

*Correspondence to: Dr. Howard R. Petty, Department of Ophthalmology and Visual Sciences, 1000 Wall Street, The University of Michigan Medical School, Ann Arbor, MI 48105, USA

Email: hpetty@umich.edu

Published online 31 August 2010 in Wiley Online Library (wileyonlinelibrary.com)

DOI: 10.1002/cyto.a.20961

Abstract

Kinetic studies of nicotinamide adenine dinucleotide phosphate autofluorescence have been conducted in adherent neutrophils using an improved microscopic photometry system incorporating low noise excitation and detection systems. Dynamic autofluorescence oscillations were found with periods ranging from ~4 min to ~10 s. The largest portion of the population of oscillating neutrophils (32%) had periods near 2 min. The next largest group at 25% exhibited periods of 1 min or less. These oscillations could not be accounted for by instrument artifacts, cell shape changes away from the focal plane, or other factors. They disappeared when detergent was added to oscillating cells. Higher-frequency oscillations disappeared as cells changed shape, indicating a correlation between these two processes. This approach provides a reliable method to monitor this cellular property. © 2010 International Society for Advancement of Cytometry

Key terms

microfluorometry; autofluorescence; cell shape; metabolism

MICROSCOPE-based photometry measurements, especially quantitative measurements of fluorescence intensities, have been used for many years to study cell-associated labels or reaction product formation using fluorescence or absorption techniques (1). In addition to the application of exogenous substances to cells and tissues, endogenous cellular materials can also be quantified using photometric tools, such as NADH autofluorescence. Microphotometry has also been extensively used to monitor dynamic changes within living cells based on the intensity of intracellular dyes using ratiometric methods, such as in calcium and membrane potential measurements. Ratioing corrects for systematic sources of error, including lamp fluctuations, dye loss, and sample thickness. For neutrophil metabolism studies, it is difficult to calculate the NADH/flavoprotein ratio because the mitochondrial flavoprotein intensity is low and irrelevant flavoproteins, such as the nicotinamide adenine dinucleotide phosphate (NADPH) oxidase (2), are present. It is possible to ratio NADH fluorescence (470 nm) relative to a wavelength that is insensitive to metabolic activity, 415 nm (3), which controls for factors such as lamp fluctuations and cell shape/thickness changes.

To measure the intensity of comparatively weak NAD(P)H autofluorescence, it is important to remove as much noise from the system as possible. Previously, our group developed a super-quiet microfluorometry system, which uses a single-photon counting system in conjunction with a feedback-regulated super-quiet mercury–xenon lamp driven by a highly stabilized power supply (4). Although this system works very well in most cases, including NAD(P)H detection in tumor cells, the ultraviolet intensity is not ideal for the detection of NAD(P)H autofluorescence in neutrophils. We have, therefore, used an ultraviolet light-emitting diode (UVILED) as a highly stable light source. This approach enabled us to conduct a quantitative survey of neutrophil NAD(P)H autofluorescence oscillations and to perform 450 nm/410 nm ratiometric analyses.

Materials and Methods

Materials

Phosphate buffered saline and low-intensity blue-fluorescent beads were obtained from Invitrogen Corp. (Carlsbad, CA). Cover-glass bottom dishes were purchased from MatTek Corporation (Ashland, MA). Unless otherwise noted, chemicals were obtained from Sigma-Aldrich Chemical Company (St. Louis, MO).

Isolation of Human Neutrophils

Peripheral blood was collected from healthy male and female donors in compliance with the guidelines of the University of Michigan Institutional Review Board for Human Subject Research. Neutrophils were isolated from peripheral blood using Ficoll-Histopaque density gradient centrifugation (Sigma-Aldrich Chemical Co.). Samples were resuspended and then washed in phosphate buffered saline by centrifugation. After washing, cells were suspended in imaging buffer (5) and placed in cover-glass bottom dishes.

To provide a negative control, some purified neutrophils were kept *in vitro* for 2 days before experiments to promote spontaneous apoptosis and cell death. In other cases, neutrophils were fixed with a modified dithiobis(succinimidyl propionate) procedure (6). In brief, cells were first fixed using dithiobis(succinimidyl propionate) (1 μg/mL; Pierce, Rockford, IL) in Hank's balanced salt solution for 10 min at room temperature. Cells were washed and then fixed a second time with 3.7% paraformaldehyde (Sigma-Aldrich Chemical Co.). Dead cells did not display motility or any normally observed movement, such as pseudopodia extension.

Microfluorometry System

NAD(P)H autofluorescence was detected with microfluorometry using a system similar to that previously described (4). As illustrated in Figure 1, light was delivered from a continuous UVILED (365 nm) (Rapp OptoElectronic, Hamburg, Germany) to a Zeiss microscope via a liquid light guide. Light was delivered to the sample using a 365WB50 excitation filter and a 400-nm dichroic long-pass mirror (Chroma Technology Corp., Rockingham, VT). Samples were viewed using a 100×/numerical aperture 1.3 objective. A D-104 microscope photometer (Photon Technology International [PTI], Birmingham, NJ), containing a 450DF30 emission filter, was connected to a refrigerated PMT housing (Products for Research, Danvers, MA) containing an R1527P photon-counting photomultiplier tube (Hamamatsu Corp., Bridgewater, NJ). An adjustable diaphragm was used to exclude other cells from the measurements and minimize the background intensity levels. All experiments were performed

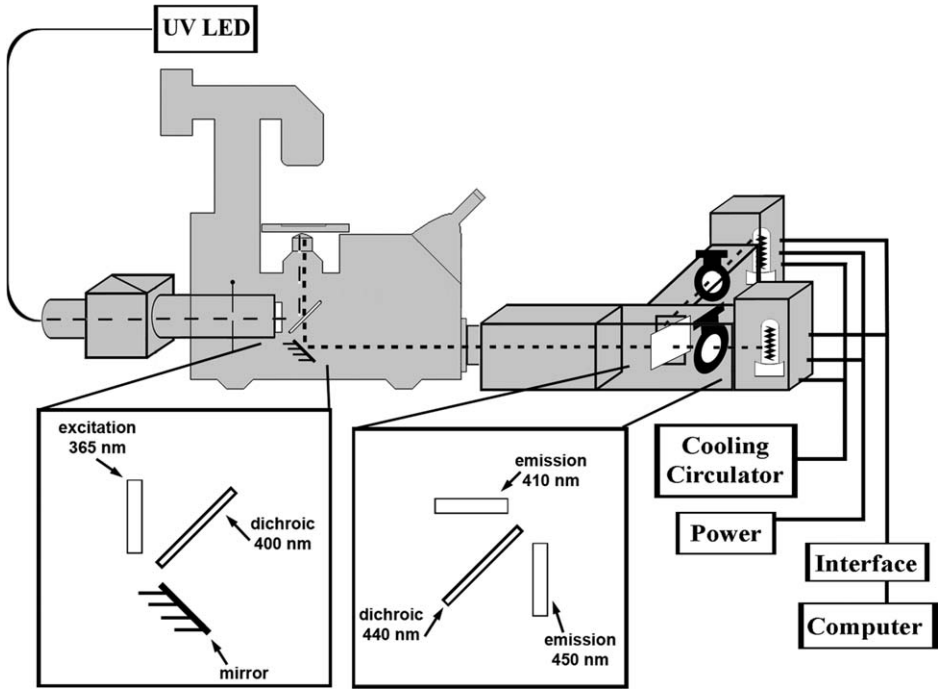

Figure 1. Microscope system diagram. A continuous ultraviolet light emitting diode (UVILED, 365 nm) source was attached to a Zeiss microscope via a liquid light guide. The light path is represented with a dashed line. The inset diagrams illustrate the configurations of filters and mirrors. Light was delivered to the sample using a 365WB50 excitation filter and a 400-nm dichroic long-pass mirror (Chroma Technology Corp., Rockingham, VT). The signal was detected with a D-104 microscope photometer, containing a 440-nm dichroic reflector, a 450DF30 emission filter, and a 410-nm emission filter. Each emission pathway terminated at a refrigerated PMT housing containing a Hamamatsu R1527P photon-counting photomultiplier tube. For nonratiometric experiments, the 440-nm dichroic reflector was removed. An adjustable diaphragm was used to exclude other cells from the measurements. The attached computer used Felix software to collect and process data. All experiments were performed in a dark room within an aluminum enclosure with the microscope stage set to 37°C.

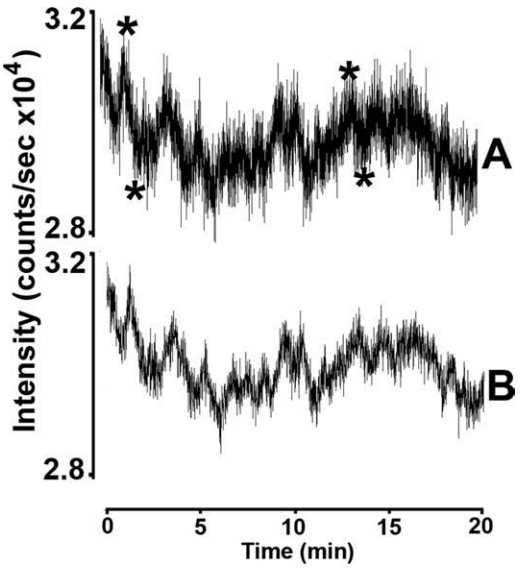

Figure 2. Data processing. Data were recorded at four points per second. Recordings are plotted in real time as intensity in counts per second versus time (min). Trace **A** shows raw data collected from one recording. *P* values were calculated for adjacent peak and trough pairs using raw data (trace A, asterisks). The *P* value was found to be less than 0.0001 for both pairs shown. Each recording was then filtered using the Savitzky—Golay smoothing equation, with a buffer size of 7. The result of the smoothing function is shown as trace **B**.

in a dark room within an aluminum enclosure with the microscope stage set to 37°C.

To control for intensity changes independent of cell metabolism, such as illumination intensity changes or cell shape/thickness changes, emission intensities at 450 and 410 nm were recorded (3). For emission ratioing studies, a second identical PMT and refrigerated PMT housing were connected to the microscope photometer. A 440-nm dichroic mirror was inserted in the photometer to permit simultaneous emission measurements at two wavelengths. A 450DF30 optical filter (to detect NAD(P)H autofluorescence) and a 3^{RD} millennium 400–420 nm discriminating filter (Omega Optical, Brattleboro, VT), to detect changes in emission intensity independent of cell metabolism, were used.

Data Acquisition and Analysis

Dishes containing neutrophils in imaging buffer were placed on a heated microscope stage and then were photographed to document cell shape. Single-cell autofluorescence was recorded with a photomultiplier tube at four points per second in 20-min segments using FeliX software (PTI). In some cases, fluorescent beads, with excitation and emission properties similar to NAD(P)H were used. To minimize Brownian motion during observations, the beads were placed on slides, covered in low-melting-point agarose at 45°C, then covered with a cover slip, and allowed to cool. After recording experiments and controls, *P* values were calculated comparing 10 consecutive raw data points at an oscillation peak with 10 consecutive data point at the following trough (GraphPad software). Traces were smoothed in FeliX software by the Savitzky–Golay function (7) with a buffer size of 7, as illustrated in Figure 2.

Results

Comparison of Light Sources

A leading source of noise in photometric measurements is the fluctuation and drift of the excitation light. To minimize this noise, we tested a light-emitting diode (UVILED) in microphotometry experiments. Figure 3 shows a representative comparison of emission measurements collected using a

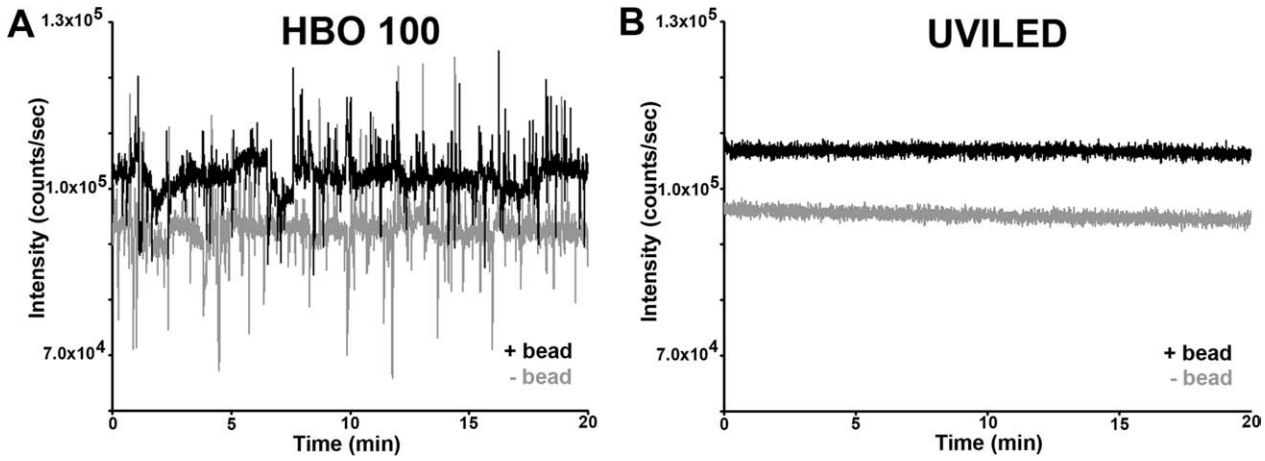

Figure 3. Lamp stability. The performance of a UVILED lamp was compared with that of a standard HBO 100 mercury lamp. Recordings were made on blank cover slips and single immobilized low-intensity blue fluorescent beads for each source. Photomultiplier tube gain was reduced for HBO 100 lamp recordings to equalize the blank intensity reading for both lamps near 1×10^5 counts per second. A blank recording with the HBO 100 light source yields an intensity of $9.27 \times 10^4 \pm 4.74 \times 10^3$ counts per second (**A**, gray trace), whereas the UVILED gives an intensity of $9.52 \times 10^4 \pm 8.42 \times 10^2$ counts per second (**B**, gray trace). Similarly, recordings of single beads resulted in an intensity of $1.02 \times 10^5 \pm 3.65 \times 10^3$ counts per second for the HBO 100 (A, black trace), and an intensity of $1.07 \times 10^5 \pm 7.05 \times 10^2$ counts per second for the UVILED source (B, black trace) ($n = 3$).

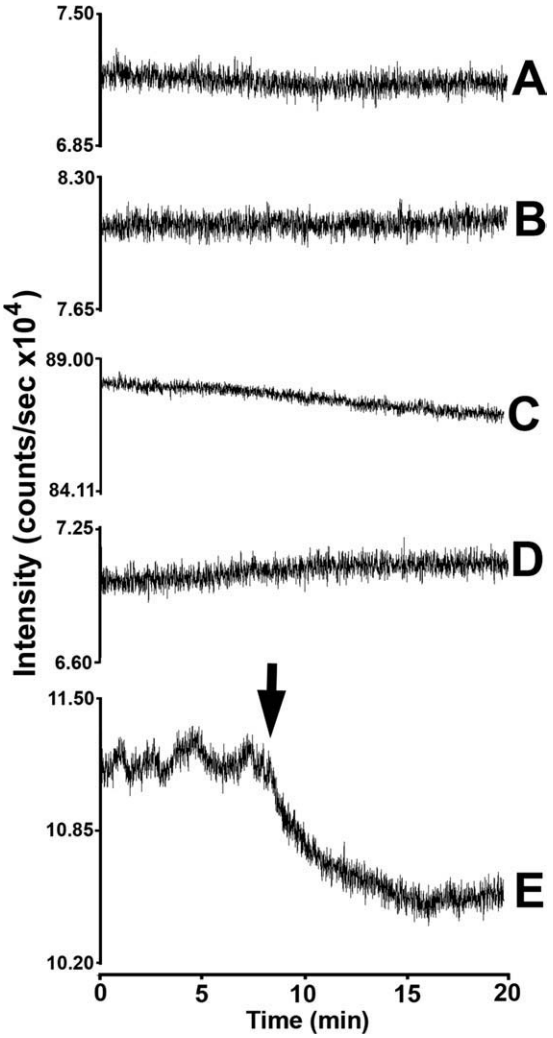

Figure 4. Kinetic studies of fluorescence. To characterize the nature of NAD(P)H autofluorescence, a series of control experiments were carried out. Each control experiment was conducted on a 37°C heated stage over a 20-min time interval. Trace **A** is a PMT recording with no dish or slide in place. Trace **B** is a recording with a blank dish. Immobilized dim blue fluorescent beads were recorded in trace **C**. The signal from a dead neutrophil was recorded in trace **D**. In trace **E**, a live oscillating neutrophil was used. During recording, 1% Triton-X 100 solution was added to lyse the cell (at arrow), confirming that the oscillations stop on death of the cell (A—E, $n = 3$).

UVILED light source and a standard HBO 100 mercury lamp. To provide a fair comparison at similar shot noise levels, the excitation levels were adjusted to give similar emission intensities. Readings were made with each light source using a blank cover slip or with a single immobilized fluorescent bead as the sample. A blank recording with the HBO light source gave a background intensity of $9.27 \times 10^4 \pm 4.74 \times 10^3$ counts per second (Fig. 3A, gray trace). In contrast, using the UVILED source resulted in an intensity reading of $9.52 \times 10^4 \pm 8.42 \times 10^2$ counts per second (Fig. 3B, gray trace). Similarly, recordings of single beads resulted in an average intensity of $1.02 \times 10^5 \pm 3.65 \times 10^3$ counts per second for the HBO 100 (Fig. 3A, black trace) and an average intensity of $1.07 \times 10^5 \pm 7.05 \times 10^2$ counts per second for the UVILED (Fig. 3B, black trace). As illustrated by this figure, the UVILED provides a marked fivefold reduction in noise.

Kinetic Evaluation of Fluorescence Emission

Kinetic experiments were conducted to ascertain the properties of the UVILED-based microphotometry system. Figure 4 shows representative examples of kinetic experiments, which were performed at 37°C and recorded at four points per second over 20-min time intervals using an excitation wavelength of 365 nm and an emission wavelength of 450 nm. Photometer recordings were conducted with an empty stage, a blank dish, and an immobilized dim blue fluorescent bead (Figures 4A–4C). Although the instrument was set-up to record data, no signal was observed using an empty stage or blank dish. A signal was observed for blue fluorescent beads (Fig. 4C shows the emission from one bead), although this intensity declined slightly over time. These experiments did not yield detectable oscillations.

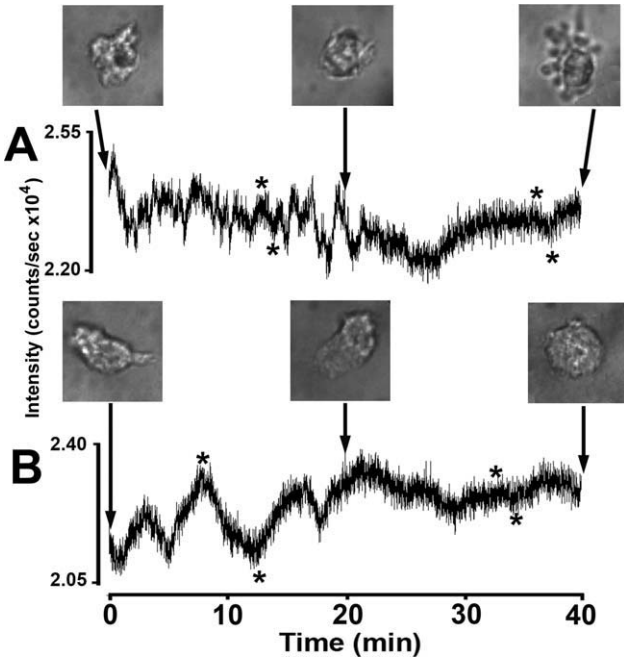

Figure 5. Metabolic oscillations in living human neutrophils. NAD(P)H autofluorescence oscillations are observed in human neutrophils. Traces A and B show two different cells recorded over a 40-min time period. White light images of the cells are shown at 20-min intervals (arrows). The cell in trace **A** maintains an oscillatory period of ~1 min for over a 20-min time interval ($P < 0.0001$, first asterisk pair at the left side); then, the oscillations increase markedly in period and decrease in amplitude ($P = 0.2543$, second asterisk pair on the right side). During this time period, cell A also changes from a polarized (0 min) into a more spherical (40 min) shape with numerous extensions. In trace **B**, the cell begins the recording with oscillations of a period of ~4 min. These oscillations continue for about 30 min; then, amplitude markedly decreased ($P < 0.0001$ for first asterisk pair; $P = 0.9878$ for second asterisk pair). Like cell A, cell B also changes shape from highly polarized at 0 min into a spherical shape at 40 min. These data are representative of 26 recordings taken of 19 cells over 9 separate days.

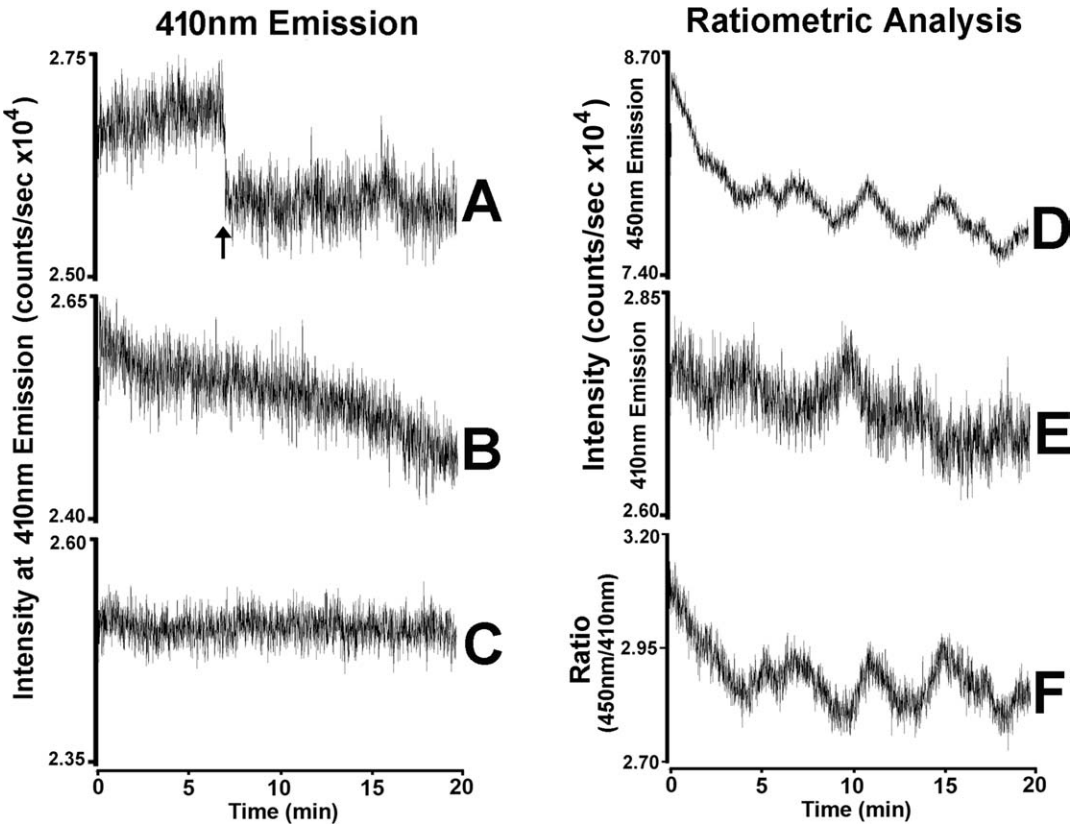

Figure 6. Intensity ratioing studies. To control for intensity changes unrelated to cell metabolism, emission ratios were calculated using autofluorescence emissions of 450 nm for NAD(P)H and 410 nm to detect dynamic changes in focus, lamp intensity, cell thickness, and cell shape. Traces A—C record the emission of single cells at 410 nm. Trace **A** shows an example of an abrupt change in the illumination intensity (arrow), which occurred in 7% of the samples. Trace **B** shows a gradual drift in 410 nm emission intensity likely related to changes in cell shape (36% of the recordings), whereas trace **C** shows no obvious change in 410 nm emission (44% of the recordings). Traces D—F show an example of the ratiometric analysis of a single cell. Traces **D** and **E** were recorded simultaneously, and then divided (450 nm/410 nm) to produce the ratio trace **F**. Oscillating NAD(P)H autofluorescence is shown in trace D (450 nm), whereas the ratio control (410 nm), also exhibiting some oscillation, is shown in trace E. Of all the samples, oscillations at 410 nm were observed in 16% of the recordings. After controlling for cell thickness, the calculated ratio (450 nm/410 nm) in trace F shows prominent oscillations. All traces were smoothed using the Savitzky—Golay function, with a buffer size of 7. Note that the ordinates differ. These experiments were repeated on 45 cells over 9 days of experimentation.

Thus, instrument artifacts, such as oscillations in illumination intensity, could not explain the results described below.

We next examined cellular properties using the microphotometry system. Kinetic microphotometry experiments were performed on expired cells. Neutrophils were isolated and prepared as described in the Materials and Methods section. Figure 4D is a representative example of a neutrophil after 2 days *in vitro*; no signals or oscillations were noted because these cells rapidly become apoptotic *in vitro*. Similarly, after chemical fixation, no kinetic features were apparent (data not shown). To further test the nature of cell autofluorescence, experiments were performed in which live neutrophils were treated with detergent (e.g., Fig. 4E). During the recording, Triton-X 100 was added to the dish at a final concentration of 1%, thereby lysing the cell (Fig. 4E, arrow). After detergent addition, the oscillations stopped suddenly, and the overall autofluorescence intensity decreased (Fig. 4E). These studies demonstrate that the mechanism responsible for autofluorescence oscillations requires living cells with an intact cell membrane.

Properties of Autofluorescence Oscillations in Live Human Neutrophils

We next characterized the properties of live cell autofluorescence oscillations. Single-cell autofluorescence experiments at the NADH excitation and emission maxima were recorded as described above. Figure 5 shows two examples of the dynamic oscillations observed. Figure 5A follows a cell exhibiting oscillations with a ~1-min period, which persist for over 20 min, before slowing markedly. During this time period, the cell of Figure 5A also changes from a morphologically polarized shape to a round shape with numerous protrusions (Fig. 5A). Figure 5B shows a cell that begins the recording exhibiting large amplitude oscillations with a period of ~4 min. These oscillations persist for nearly 30 min, with the amplitude dramatically decreasing after 25 min. Like the cell in Figure 5A, the cell in Figure 5B also undergoes changes in shape from being highly polarized at 0 min, to being circular and flat at 40 min (Fig. 5B). In fact, although oscillations are still visible, both cells showed enough of a decrease in

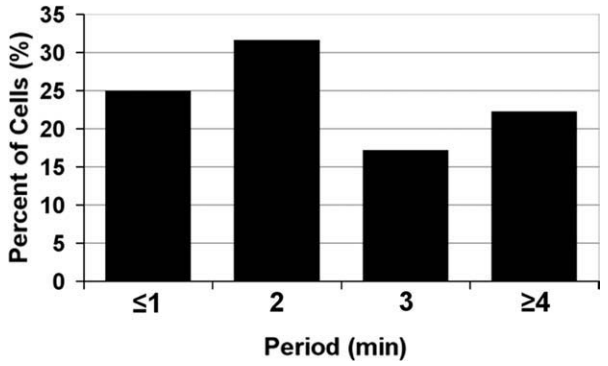

Figure 7. Quantitative analysis of metabolic oscillations within a population of human neutrophils. A population of oscillating neutrophils was analyzed by recording cells as described above, and then the periods were determined for each trace. The results were plotted by period (in min) vs. percentage of cells. The distribution of oscillatory periods is as follows: 25% of cells had a period of 1 min or less, 32% had a period of ~2 min, 17% had a period of ~3 min, and 22% had periods of 4 min or longer. This represents a compilation of 246 recordings on 207 different cells collected over 64 separate days.

amplitude for the oscillations to lose statistical significance (Fig. 5, asterisk pairs at ~10 vs. ~35 min). Within the population of cells studied, cells that became more rounded showed an increase in period (16 recordings), becoming more highly polarized resulted in a decrease in period (seven recordings), and if no perceptible change in cell shape is made, the period remained the same (three recordings). These results were consistent with earlier findings suggesting that metabolic oscillations correlate with cell shape (8), and discontinue when neutrophils return to a resting or circular shape.

Emission Ratioing Experiments

To provide another specificity control for intensity changes independent of cell metabolism, such as changes in lamp intensity or cell shape/thickness change, emission ratios were calculated using autofluorescence emissions of 450 nm for NAD(P)H, and 410 nm for non-NAD(P)H intensity (3). We first characterized the emission properties of neutrophils at 410 nm (Fig. 6). Traces A–C show the various types of kinetic intensity traces observed. These include an abrupt change in emission intensity, likely because of a change in illumination intensity (arrow), a gradual drift in intensity, and an unchanging intensity at 410 nm; the latter was observed most often. In infrequent cases, the intensity at 410 nm was observed to oscillate (trace E). The traces in Figures 6D–6F show a ratiometric analysis of a single cell. Traces D and E are recorded simultaneously, and then divided (450 nm/410 nm) to produce the ratio trace F. Oscillating NAD(P)H autofluorescence is shown in trace D (450 nm) and in the intensity ratio (trace F). Thus, changes in cell thickness, as judged by the calculated ratio (450 nm/410 nm), cannot account for these oscillations.

NAD(P)H Oscillation Heterogeneity

Over the course of these studies, the oscillation periods of many different neutrophils were analyzed as described above. The periods of these oscillations were categorized, and then plotted as a percentage of the total number of cells. The distribution of oscillatory periods is shown in Figure 7. The greatest number of cells had periods near 2 min (32%), followed by cells with periods of 1 min or less (25%). Cells with periods near 3 min made up 17% of the population, whereas cells with periods of 4 min or more accounted for 22%. The variation in oscillatory periods in this neutrophil population extends previous studies.

Discussion

The overall performance of the photometry system described above is excellent. The UVILED source was found to be superior to a conventional mercury lamp. Using the UVILED system, the standard deviation in the measured intensity was found to be about three times greater than the expected shot noise of photon emission. Consequently, it is possible to detect changes in intensity, such as oscillations, at a high level of statistical significance.

Metabolic oscillations have been observed in several cell types, including yeast, neutrophils, pancreatic islet cells and, recently, rat basophilic leukemia and human hepatocellular carcinoma cells (9–15). In this study, we have improved on the detection of these oscillations, especially, their detection in weakly fluorescent neutrophils. As these oscillations correlate with cell activities, such as shape change, they are of considerable physiological interest.

Using a variety of experimental approaches, we have rigorously excluded the possibility of systematic instrument artifacts, such as lamp oscillations. Because the axial resolution under the illumination conditions used is about 1.5 μm, it remained possible that cell movement out of the plane of focus caused changes in NAD(P)H autofluorescence. Therefore, we monitored fluorescence emission at the metabolically relevant wavelength of 450 nm and at 410 nm (3). These data indicate that autofluorescence oscillations at 450 nm cannot be explained by axial changes in cell shape. Thus, instrument features and biological measurements indicate that the oscillations are of a biological nature.

A recent study suggests a role for neutral sphingomyelinase (N-SMase) in cell shape and cellular migration (16). Interestingly, the perturbation of N-SMase and its downstream lipids greatly influence cell shape. Because we have observed a strong correlation of NAD(P)H oscillation period and cell shape, we are particularly interested in exploring the relationship between metabolic oscillations and the translocation of N-SMase to the neutrophil membrane and its consequent effects on cell shape and signal transduction.

Literature Cited

1. Ploem JS. Quantitative fluorescence microscopy. In: Meek GA, Elder HY, editors. Analytical and Quantitative Methods in Microscopy. Cambridge, UK: Cambridge University Press; 1977. pp 55–89.
2. Roos D, Balm AJM. The oxidative metabolism of monocytes. In: Sabarra AJ, Strauss RR, editors. The Reticuloendothelial System: A Comprehensive Treatise, Vol. 2. New York, NY: Plenum Press; 1980.
3. White RL, Wittenberg BA. NADH fluorescence of isolated ventricular myocytes: Effects of pacing, myoglobin, and oxygen supply. Biophys J 1993;65:196–204.
4. Clark AJ, Petty HR. Super-quiet microfluorometry: Examples of tumor cell metabolic dynamics. In: Mendez-Vilas A, Diaz J, editors. Modern Research and Educational Topics in Microscopy, 2007 ed., Vol. 1. Spain: Formatex; 2007. pp 403–408.

5. Clark AJ, Petty HR. Observation of calcium microdomains at the uropod of living morphologically polarized human neutrophils using flash lamp-based fluorescence microscopy. Cytometry Part A 2008;73A:673–678.
6. Safiejko-Mroczka B, Bell PB Jr. Bifunctional protein cross-linking reagents improve labeling of cytoskeletal proteins for qualitative and quantitative fluorescence microscopy. J Histochem Cytochem 1996;44:641–656.
7. Savitzky A, Golay MJE. Smoothing and differentiation of data by simplified least squares procedures. Anal Chem 1964;36:1627–1639.
8. Petty HR, Kindzelskii A, Espinoza J, Romero R. Trophoblast contact de-activates human neutrophils. J Immunol 2006;176:3205–3214.
9. Ghosh A, Chance B. Oscillations of glycolytic intermediates in yeast cells. Biochem Biophys Res Commun 1964;16:174–181.
10. Richard P, Bakker BM, Teusink B, Van Dam K, Westerhoff HV. Acetaldehyde mediates the synchronization of sustained glycolytic oscillations in populations of yeast cells. Eur J Biochem 1996;235:238–241.
11. Amit A, Kindzelskii A, Zanoni J, Jarvis JN, Petty HR. Complement deposition on immune complexes reduces the frequencies of metabolic, proteolytic, and superoxide oscillations of migrating neutrophils. Cell Immunol 1999;194:47–53.
12. Vern BA, Shuette WH, Leheta B, Bern JC, Radulovaki M. Low-frequency oscillations of cortical oxidative metabolism in waking and sleep. J Cereb Blood Flow Metab 1988;2:215–226.
13. Chen R, Chen JY, Zhou LW. Metabolic patterns (NAD(P)H) in rat basophilic leukemia (RBL-2H3) cells and human hepatocellular carcinoma (Hep G2) cells with autofluorescence imaging. Ultrastruct Pathol 2008;32:193–198.
14. Luciani DS, Misler S, Polonsky KS. Ca^{2+} controls slow NAD(P)H oscillations in glucose-stimulated mouse pancreatic islets. J Physiol 2006;572(Pt 2):379–392.
15. Imai SI. "Clocks" in the NAD World: NAD as a metabolic oscillator for the regulation of metabolism and aging. Biochim Biophys Acta 2010;1804:1584–1590.
16. Sitrin RG, Sassanella TM, Petty HR. An obligate role for membrane-associated neutral sphingomyelinase activity in orienting chemotactic migration of human neutrophils. Am J Resp Cell Mol Biol (in press).